Antagonism of Tachykinin receptor 1 promotes Foxp3$^+$ regulatory CD4 T cells and controls gut mucosal inflammation

Girdhari Lal

glal@nccs.res.in

National Centre for Cell Science https://orcid.org/0000-0002-3799-3603

Amrita Mishra

National Centre for Cell Science

Surojit Karmakar

National Centre for Cell Science

Namrita Halder

National Centre for Cell Science

Mir Habib

National Centre for Cell Science

Dharmendra Kumar

Armed Forces Medical College

Article

Keywords: Neurokinin receptor, Substance P, Regulatory T cells, Neuroimmune communication

Posted Date: March 28th, 2024

DOI: https://doi.org/10.21203/rs.3.rs-4105036/v1

Additional Declarations: There is **NO** Competing Interest.

Abstract

Neuroimmune communication of the enteric nervous system (ENS) in gut-associated lymphoid tissues helps to maintain the delicate balance between gut inflammation and tolerance. Substance P (SP) is a neuropeptide neurotransmitter produced by ENS and enteroendocrine cells, lymphocytes, gut macrophages, and brain neurons. SP binds to tachykinin receptors (TACRs, also known as neurokinin receptors). Inflammatory bowel disease (IBD) and irritable bowel syndrome (IBS) patients are known to have altered TACRs expression and strongly correlate with the pathogenesis of these diseases. How SP-TACR interaction modulates the differentiation and function of inflammatory CD4 T cells (Th1, Th17) and regulatory CD4 T cells ($Foxp3^+$Tregs and Th2 cells) during gut inflammation and autoimmunity is unclear. We showed that among the various subsets of CD4 T cells, splenic $Foxp3^+$Tregs and Th17 cells had the highest expression of TACRs. Agonizing the TACR1 with SP in the dextran sodium sulfate (DSS)-induced colitis in mice exacerbated the disease severity, which was inhibited by treatment with a TACR1-specific antagonist. TACR1 antagonist promoted the differentiation of $Foxp3^+$ Tregs cells, and Tregs induced in the presence of TACR1 antagonist showed an increased expression of LAP1, PD-L1, CD62L, Helios, and CD73 molecules. They suppress the proliferation of effector CD4 T cells and control skin and gut inflammation. We showed that antagonizing the TACR1 signaling promotes $Foxp3^+$ Tregs and controls skin and gut inflammation. Our data suggest that antagonizing the TACR1 provides a clinical advantage in preventing gut inflammation and colitis.

Introduction

Neuroimmune communication is the bidirectional crosstalk between the nervous and immune systems. These communications are either maintained by direct cell-to-cell contact or through neurotransmitters. Several studies suggested the involvement of neuro-immune communications in different autoimmune diseases (1–5). Immune cells express wide arrays of neurotransmitter receptors, allowing them to respond to signals from neuronal circuits in the tissue microenvironment (5). Neuroimmune communication of the enteric nervous system plays a crucial role in relaying psychological stress to intestinal inflammation and colitis. Among the several neurotransmitters, tachykinins (also known as neurokinins) have been linked to pain, inflammation, cancer, depression, gut function, hematopoiesis, sensory processing, and hormone regulation (1, 6). The *tac* gene encodes the major tachykinin family members and gives rise to substance P (SP), neurokinin A (NKA), neurokinin B (NKB), neuropeptide K (NPK), and neuropeptide-γ (NP-γ) (6). SP is one of the prominent members of the tachykinin family and is identified as the first of many ‘brain-gut neuropeptides’ and binds to its receptor known as the tachykinin receptors (TACRs) or neurokinin receptors (NKRs) (6). SP is expressed by enteric neurons and enterochromaffin cells, and nerves in the brain and is known to control various physiological functions (7). Tachykinin receptors (TACRs) are G protein-coupled receptors encoded by the *tacr* gene and have three different types (TACR1, TACR2, and TACR3) that bind to its ligand SP (6). TACR1 is expressed on T and B cells, macrophages in the Peyer’s patch, and spleen and is crucial in modulating immune responses (1, 8). TACR2 is mainly expressed by myocytes, neuronal varicosities, and epithelial cells,

whereas TAR3 is primarily localized in the neuronal compartment (6). SP-expressing nerve fibers are present at the dermis and epidermis as well as innervate the dermal blood vessels, keratinocytes, mast cells, DC, and hair follicles, and respond to various external stimuli (heat, ultraviolet light, allergen, and scratching) or internal stimuli (cytokines, proteases, and prostaglandins) (6).

In humans, activated T cells express the preprotrachykinin (*PPTA*) gene, which transcribes and translates into inactivated-SP, which is further processed by an enzyme peptidyl glycine α-amidating monooxygenase (PAM) to form activated-SP (1). An enzyme called angiotensin-converting enzyme (ACE) degrades the circulating SP. The resting T cells do not express SP or TACRs (9). Activated T cells in rodents also synthesize SP and modulate T cell response in an autocrine manner (10). TACR signaling has been shown to have increased disease-enhancing effects in psoriasis (11, 12), rheumatoid arthritis (13, 14), inflammatory bowel disease (IBD) (15, 16), and other inflammatory diseases (1). TACR1 expression is strongly associated with the grade of IBD and its tissue distribution in the lamina propria mononuclear cells, epithelium, submucosal vasculature, and smooth muscle in the colon (17–19).

CD4 T cells are vital in maintaining gut homeostasis and orchestrating immune responses in the gut and other gut-associated organs. However, TACR1 expression of Treg or Th17 cells alters the pathophysiology of gut inflammation is less clear. A recent study found that simultaneous TACR1 and TCR activation is required for Ca^{+2}-dependent TCR signaling and T cell survival, particularly in Th1 and Th17 cells (20). TACR1 antagonist aprepitant and its pro-drug fosaprepitant are approved for clinical use to control chemotherapy-induced nausea and vomiting and postoperative nausea and vomiting (21). A phase II clinical trial with dual TACR1/TACR2 antagonist DNK333 in women with diarrhea-predominant IBS showed relief with symptoms compared to control (22). However, the detailed molecular mechanism of TACR1-antagonism and control of gut inflammation is not well characterized. Th1 and Th17 cells play an important role in controlling gut inflammation and autoimmunity (23, 24) and other autoimmune diseases. However, little is known about how tachykinin signaling affects the differentiation and function of CD4 T cells under various physiological and pathophysiological conditions in the gut. Furthermore, how the TACR1 antagonist controls different effectors and regulatory CD4 T cells is not known.

Our findings show SP synthesizing enzymes and its cognate receptors on various subsets of CD4 T cells, including Th2, Th17, and Tregs. Furthermore, antagonizing the TACR1 reduced the severity of colitis and prevented the pathological alteration in the colon. While looking into these phenomena in more detail, we found that TACR1 antagonist treatment increased the frequency and suppressive capacity of $Foxp3^{+}$ Tregs *in vivo* and *in vitro* and controlled gut inflammation. Antagonizing the TACR1 during Treg differentiation showed several suppressive markers and inhibited the proliferation of effector CD4 T cells. Further adoptive transfer of TACR1-antagonist treated induced Tregs showed protection from naïve CD4 T cell-induced skin and gut inflammation in immunocompromized NRG mice (lack T cells, B cells, and NK cells).

Results

Various subsets of CD4 T cells express TACR1 expression

The abundance of tachykinin receptors in the gastrointestinal mucosa and submucosa has been linked to a critical role in maintaining gut homeostasis (25, 26). Our results showed that all three TAC receptors (TACR1, TACR2, and TACR3) mRNAs were expressed in the secondary lymphoid organs (spleen, mesenteric lymph nodes, and Peyer's patches) under homeostatic conditions (Fig. 1A). Further, analysis of purified Th17 cells ($CD4^+$ $Foxp3rfp^-RORγtgfp^+$) and natural Tregs (nTregs; $CD4^+$ $Foxp3rfp^+RORγt$-GFP^-) in the spleen showed increased TACRs mRNA expression, whereas naïve CD4 T cells ($CD4^+CD25^-Foxp3rfp^-CD44^-$) and memory CD4 T cells ($CD4^+CD25^-Foxp3gfp^-CD44^+$) had minimal expression **(Fig. 1B)**. To understand more details on the expression (mRNA) of TACRs on various subsets of CD4 T cell subsets (Th1, Th2, Th17, and Tregs), naïve $CD4^+$ T cells were *in vitro* differentiated into various CD4 T subsets **(Figure S1)**. Among them, Th2 cells had the highest expression of TACR mRNA among the various subsets of CD4 T cells **(Fig. 1C).** However, protein expression of TACR1 was highest in the cultured Th17 cells (Fig. 1D). Furthermore, TACR1 expression was also seen on the naïve CD4 T cells ($CD4^+CD25^-CD44^-CD62L^+$), memory cells ($CD4^+CD25^-CD44^+$), Th1 ($CD4^+$T-bet^+), Th2 ($CD4^+GATA3^+$), Th17 cells ($CD4^+RORγt^+$), $RORγt^+Foxp3^+$ cells and natural Tregs (nTregs; $CD4^+Foxp3^+$) in the Peyer's patch (Fig. 1E), and lamina propria (**Figure S1B**).

To understand the CD4 T cell-intrinsic metabolism of substance P, we investigated the expression of PPTA, PAM, and ACE genes in the various subsets of CD4 T cells. Among the various subsets, Th2 cells showed the highest PPTA and PAM gene expression (genes responsible for the formation of active substance), whereas Th1 cells showed low ACE expression (SP degrading enzyme) among various subsets of CD4 T cells **(Fig. 1F)**. Together, these results suggest that Th2 cells express the highest expression of TACRs and enzymes required for SP synthesis compared to activated CD4 T cells (Th0), Th1, Th17, and Tregs. Analysis of culture supernatants showed expression of SP under various T cell differentiation conditions **(Figure S1C)**. These findings suggest that CD4 T cells express a tachykinin system in various CD4 T cells in different lymphoid tissues.

Antagonizing the TACR1 reduces the severity and pathology of inflammatory colitis

CD4 T cells play an important role in gut inflammation and autoimmunity (23, 24, 27). To understand the importance of SP in gut inflammation, C57BL/6 mice were given dextran-sodium sulfate (DSS; 2% w/v) in drinking water and injected (i.p.) TACR1-specific agonist SP [(Sar9, Met(O2)11)-Substance P (trifluoroacetate salt)] or TACR1 antagonist (CP96345) or vehicle as control, and monitored the body weight loss and disease activity index daily. Our results showed that DSS-treated mice that received SP resulted in severe body weight loss **(Fig. 2A)** and a significantly increased clinical disease activity index (DAI) (Fig. 2B) compared to the control group. Treatment with SP alone did not show any weight loss (Fig. 2A**)**. To understand the effect of SP on gut inflammation, mice were given an intraperitoneal injection of TACR1-specific, a potent and non-peptide antagonist (CP-96345; 2.5 mg/kg of the mouse,

twice daily) and DSS containing drinking water (28). Our results showed that injection of CP-96345 significantly reduced weight loss **(Fig. 2A)**, disease activity index **(Fig. 2B)**, and mortality of mice **(Fig. 2C)**. CP96345 treatment also restored the colon length, which was reduced with DSS treatment **(Fig. 2D)**. Histopathological examination of the colon by H&E staining showed that CP96345 treatment reduced pathology as well as infiltration of mononuclear cells **(Fig. 2E)**. We further investigated the role of other TACRs, TACR2 and TACR3, on gut inflammation. Our results showed that the TACR2 antagonist (MEN10673) is also effective in preventing colitis in the initial stage of the disease but did not show sustained protection **(Figure S2A** and **S2B).** However, treatment with a selective TACR3 antagonist, Osanetant, did not prevent the DSS-induced gut inflammation and clinical disease activity index **(Figure S2C** and **S2D)**. Furthermore, to understand the expression profile of TACRs in the colon of inflammatory bowel disease (IBD) patients, irritable bowel syndrome (IBS) patients, or in non-IBD/IBS control individuals, colonic biopsy were collected, and expression of TACR1, TCAR2 and TACR3 expression was analyzed using qRT-PCR. Our data showed that patients with gut inflammation (IBD and IBS) had higher expression of TACR1 and TACR2 mRNA **(Fig. 2F)**. Expression of TACR3 mRNA was not detected in the colonic biopsies (data not shown). Together, our results showed that TACR1 is the most effective among different tachykinin antagonists, followed by TACR2 antagonists in the early stage of gut inflammation. However, TACR3 antagonism did not show any effect on colitis in mice.

DSS-induced gut inflammation shows increased TACR1 expression on CD4 T cells.

Since TACR1 antagonism significantly controls gut inflammation, we further investigated the expression of TACR1 on various subsets of CD4 T cells. C57BL/6 mice were given DSS in drinking water, and on day 10, expression of TACR1 was monitored on various subsets of CD4 T cells in the spleen, lymph nodes, Peyer's patch, and colon tissues. DSS-induced inflammation increased the expression of various TACRs mRNA in the spleen and mLN **(Fig. 3A)**. Furthermore, gut inflammation significantly increases the TACR1 expression in Th1, Th2, Th17, and Tregs in the spleen, mesenteric lymph nodes (mLN), and Peyer's patches **(Fig. 3B** and **Figure S3)**. Interestingly, in Peyer's patch, mice treated with DSS and CP96345 had reduced TACR1 expression in Th1, Th2, and Th17 cells **(Fig. 3C)**. Immunohistological analysis of the spleen showed that TACR1 expression increased significantly with DSS treatment, and its expression was significantly reduced with CP96345 treatment **(Fig. 3D**, upper panel**)**. In the colon, DSS treatment increased the TACR1 expression **(Fig. 3D**, middle panel**)** and SP levels **(Fig. 3D**, bottom panel**)**. Expression of these molecules was significantly reduced with CP96345 treatment in the tissues **(Fig. 3D)**. Together, these results showed that DSS-induced gut inflammation increases the TACR1 and SP expression in the colon, which is reduced by antagonizing the TACR1, suggesting the importance of SP and TACR1 expression in gut inflammation.

Antagonizing TACR1 reduces subsets of inflammatory Th17 cells and promotes Foxp3 $^{+}$ Tregs in colitis. Since TACRs are expressed on various subsets of CD4 T cells, we investigated how TACR1 antagonist modulates the various phenotypic profiles of the CD4 T cells during gut inflammation. To explore this, mice were given DSS in drinking water with or without TACR1 antagonist and, after ten days, monitoring the alteration in the various subsets of CD4 T cells in the spleen, Peyer's patches, and lamina propria

using multicolor spectral flow cytometry. Uniform manifold approximation and projection of dimensional reduction (UMAP) analysis of 11,657 recovered $CD4^+$T cells from Peyer's patches showed 15 distinct clusters (Fig. 4A). Cluster 4 ($CD44^{mid}ROR\gamma t^{mid}T\text{-}bet^{mid}CD4^{high}$), cluster 6 ($CD44^{high}ROR\gamma t^{high}CD4^{high}$), cluster 10 ($CD44^{mid}ROR\gamma t^{mid}T\text{-}bet^{mid}CD4^{high}$), and cluster 11 ($CD44^{high}ROR\gamma t^{high}CD4^{high}$) representing the inflammatory Th17 CD4 T cells populations, were significantly increased in DSS-treated mice, whereas these were reduced with TACR1 antagonist treatment **(Fig. 4A-4C)**. Cluster 8 ($CD4^+CD25^{high}Foxp3^{mid}CD73^{high}CD62L^{mid}LAP1^{mid}GITR^{high}$ population), representing a unique subset of Tregs, was significantly reduced with DSS treatment compared to the control group **(Fig. 4A-4C)**. The detailed phenotype of various CD4 T cell clusters and their phenotypes are given as a heatmap (Fig. 4C). The frequency of total Th1 ($CD4^+T\text{-}bet^+$), Th2 ($CD4^+GATA3^+$), Th17 ($CD4^+ROR\gamma t^+$), and Tregs ($CD4^+Foxp3^+$) did not show any significant change in the spleen **(Figure S4)**. In contrast, Peyer's patch showed a significantly increased frequency of $CCR7^+ROR\gamma t^+CD4^+$ T cells in the DSS-treated group, and this was significantly reduced with TACR1 antagonist treatment (Fig. 4D). In DSS-treated mice, the $CD4^+CD44^+$ cells exhibited increased expression of RORγt and T-bet expression, and these cells were significantly reduced with TACR1 antagonist treatment **(Fig. 4D)**. There were no significant alterations in the $CD4^+ROR\gamma t^+Foxp3^+$ cells (**Figure S5A**, upper panel); however, expression of TACR1 was significantly enhanced during DSS-induced inflammation, and it was reduced with TACR1 antagonist (**Figure S5A**, lower panel). In the Peyer's patch, DSS treatment significantly decreased the frequency of $CD4^+Foxp3^+$ Tregs, which was increased considerably with TACR1 antagonist treatment (Fig. 4D).

Various molecules are known to promote the regulatory function of CD4 T cells (29, 30). Since antagonism of TACR1 promotes Tregs and suppresses gut inflammation, we investigated the expression of various important molecules present on the $CD4^+Foxp3^+$ Tregs such as CD73, GITR, PD-1, PDL-1, CTLA4, CD62L, Helios, and LAP-1. Uniform Manifold Approximation and Projection of Dimension Reduction (UMAP) analysis of 2697 $Foxp3^+CD4^+$ Tregs showed 15 phenotypic clusters/populations (Fig. 4E left panel and **Fig. 4F)**. Cluster 13 represents $LAP1^{high}CD62L^{high}CD73^{high}$ expressing $Foxp3^+CD4^+$ Tregs and were significantly increased with TACR1 antagonist treated mice **(Fig. 4E)**. A heat map of the expression of each marker in each cell cluster/population was shown **(Fig. 4F)**. Further, our data showed a significantly increased CD73, CD62L, and LAP1 expression with TACR1 antagonist treatment on $CD4^+Foxp3^+$ Tregs in the Peyer's patch **(Fig. 4G)**. At the same time, expression of CD25, CTLA4, GITR, Helios, and PD-L1 molecules did not show any significant change on $CD4^+Foxp3^+$ Tregs in the Peyer's patch in the different treatment groups **(Figure S5B)**. Further, analysis of $CD4^+Foxp3^+$ Tregs showed that follicular regulatory T cells ($CXCR5^+PD\text{-}1^+CD4^+Foxp3^+$) (31) in the Peyer's patch were significantly increased with TACR1 antagonist treatment (**Figure S6A**). CD4 T cells in the lamina propria showed increased expression of IL-17A as well as $IL\text{-}17A^+IFN\gamma^+$, and secretion of these inflammatory cytokines was reduced with TACR1 antagonist treatment (Fig. 4H). However, no change was observed in the $IL\text{-}10^+$ and $TNF\text{-}\alpha^+$ CD4 T cell frequency (**Figure S6B**). The changes in the frequency of various cytokines (IL-10, IL-17A, IFN-γ and TNF-α)-producing CD4 T cells were not observed in the spleen and mLN between DSS and DSS plus TACR1 antagonist groups (**Figure S7**). Together, these results suggest that TACR1

antagonist treatment induces a complex set of regulatory CD4 T cells, inhibits the effector/inflammatory CD4 T cells in the Peyer's patch, and controls gut inflammation.

Antagonizing TACR1 signaling in naïve CD4 T cells promotes Foxp3 $^{+}$ Tregs.

To investigate if TACR1 specifically alters the CD4 T cell differentiation through an intrinsic signaling mechanism, naïve CD4 T cells were *in vitro* differentiated into Th1, Th2, Th17, and Treg cells in the presence or absence of SP or TACR1 antagonists, and monitored the differentiation of various CD4 T cell lineages. Our results showed that agonizing the TACRs with SP promoted the differentiation of Th1 cells (marked by T-bet expression) and Th17 (characterized by RORγt expression), whereas antagonizing TACR1 receptor promoted the differentiation of Th2 (marked by GATA3 expression) and Treg cells (marked by FoxP3 expression) **(Fig. 5A).** TACR1 antagonist alone in the absence of TGF-β did show alteration in the expression of Foxp3 **(Figure S8A).** In the presence of TGF-β, the TACR1 antagonist showed a dose-dependent differentiation of Foxp3^{+} Tregs **(Figure S8B).** TACR1 agonist alone or when combined with equal molar concentration of TACR1 antagonist did not show any effect of TACR1-antagonist induced Foxp3^{+}Treg differentiation **(Figure S8C)**. Interestingly, antagonizing TACR1 signaling during CD4 T cell differentiation inhibited the IL-17A secretion in Th17 cells and increased the IL-10 secretion in Foxp3^{+} Tregs **(Fig. 5B and 5C)**. Further, TACR1-induced increased differentiation of Tregs was not due to increased secretion of IL-10 or TGF-β in the culture, as neutralization of these molecules with anti-IL-10 mAb or anti-TGF-β mAb did not alter the TACR1-induced differentiation of Tregs (data not shown).

To understand the similar effect of TACR1 signaling operating in the differentiation of human Foxp3^{+}Tregs, naïve human CD4 T cells were purified from healthy human PBMCs and *in vitro* differentiated in Treg lineage in the presence or absence of TACR1 agonist (SP) or antagonist (CP). Our results showed that the TACR1 antagonist also promotes Foxp3^{+}Treg differentiation of human CD4 T cells (Fig. 5D**)**. Together, these results showed that TACR1 signaling in CD4 T cells facilitates the differentiation of Foxp3^{+}Tregs and suppresses the differentiation of pathogenic Th17 cells.

TACR1 antagonism promotes potent suppressive Tregs.

We further investigated if increased differentiation of Treg with TACR1 antagonism is also associated with a more potent suppressive function of Foxp3^{+} Tregs. To test this, naïve CD4 T cells (CD4^{+}CD44^{-}CD25^{-}Foxp3gfp^{-} T cells) were differentiated into Foxp3gfp^{+} iTregs in the presence of TACR1 agonist or antagonist. The TACR1 antagonist-treated Tregs showed the significantly increased expression of LAP-1, PDL-1, CD62L, helios, and CD73 molecules compared to control Treg or SP-treated Tregs **(Fig. 6A)**. Further, *in vitro*-differentiated Foxp3gfp^{+} iTregs were sorted, and their suppressive function was evaluated by monitoring the proliferation of Cell-Trace violet (CTV)-labeled effector CD4 T cells. Our results showed that Tregs differentiated in the presence of TACR1 antagonist showed a significant and potent suppressive function compared to control Tregs, agonist-treated iTregs, or nTregs **(Fig. 6B** and **Figure S9A)**. Furthermore, in the co-culture conditions, CP-treated nTreg (Foxp3-eGFP^{+} cells) induces the

differentiation of naïve CD4 T cells (Foxp3-RFP$^-$ cells) into Foxp3-RFP$^+$ iTregs in the presence of only α-CD3e and α-CD28 monoclonal antibodies (**Figure S9B**). Our data strongly suggest that CP-induced iTregs and CP-treated nTreg have strong suppressive potential and convert naïve CD4 T cells into the iTreg, driving better immunosuppressive function.

We further examined the suppressive capacity of TACR1 antagonist-treated iTreg in a mouse inflammation model. Naïve CD4 T cells (CD4$^+$CD44$^-$CD25$^-$Foxp3gfp$^-$ cells) were isolated from Foxp3gfp-transgenic mice spleen using flow cytometry, and these cells were *in vitro* differentiated into iTreg in the presence or absence of TACR1 antagonist or agonist. These iTregs (CD4$^+$CD25$^+$Foxp3gfp$^+$ cells) were sorted using flow cytometry and used for adoptive transfer, as shown in the experimental strategy **(Fig. 6C)**. Splenic naïve CD4 T cells (CD4$^+$CD25$^-$CD44$^-$CD45RB^{hi}Foxp3rfp$^-$ cells) were purified from Foxp3rfp transgenic mice using flow cytometry sorting and used for adoptive transfer to induce inflammatory model in mice. NRG mice (RAG1$^{-/-}$IL-2Rγ$^{-/-}$ mice; lack T cells, B cells, and NK cells) were given an intravenous injection of purified naïve CD4 T cells (CD4$^+$CD25$^-$CD44$^-$CD45RB^{hi}Foxp3rfp$^-$ cells) alone or along with cultured iTregs (CD4$^+$CD25$^+$Foxp3gfp$^+$) **(Fig. 6C)**. NRG mice that received naïve CD4 T cell alone showed inflammation in the skin and 20% mortality in 3 weeks **(Figs. 6D-6F)**. NRG mice that received naïve CD4 T cells together with TACR1 agonist-treated (SP-treated) Tregs showed strong skin inflammation and severe weight loss, and all mice died in 4 weeks. Mice who received control iTregs had mild skin inflammation and no mortality. In contrast, mice receiving TACR1-antagonist Tregs did not show skin inflammation or weight loss, and all mice survived **(Figs. 6D-6F** and **S9C)**. TACR1 agonist treatment also protected IL-23-induced psoriasis in the C57BL/6 mice (data not shown). These data suggest that Foxp3$^+$Treg induced by TACR1 antagonist protects the immunocompromised mice from gut and skin inflammation.

To understand the molecular alteration of adoptively transferred Tregs in the NRG mice, animals were sacrificed on day 28, and splenic CD4 T cells were analyzed using multicolor spectral flow cytometry. UMAP analysis of total splenic CD4 T cells in NRG mice between control iTregs or TACR1-antagonist-iTregs injected groups showed that CD4 T cells form 15 different discrete phenotypic clusters **(Figs. 6G and 6H)**. Some clusters (6, 10, 12, and 14) expressed Foxp3rfp and were significantly reduced in the iTreg group **(Fig. 6G**, right panel**)**. Cluster 15 represents what is significantly altered in CP-treated iTreg, having a mixer of Foxp3gfp$^+$ iTreg subset (represents transferred iTreg) and Foxp3rfp$^+$ iTreg (differentiated from the naïve CD4 T cells). Since we adoptively transferred naïve CD4 T cells isolated from Foxp3-rfp transgenic mice and transferred iTregs from the Foxp3gfp transgenic mice, we faithfully monitored the differentiation of naïve Foxp3rfp$^-$ CD4 T cells into Foxp3rfp$^+$ Tregs in NRG mice that received either control iTregs or TACR1 antagonist-iTregs. Our data showed that not only TACR1-treated Tregs (Foxp3gfp$^+$ cell) frequency in NRG mice were significantly higher, but it also converted a significant proportion of Foxp3rfp$^-$ naïve CD4 T cells into Foxp3rfp$^+$ iTregs **(Fig. 6I)**. Compared to control Tregs, TACR1-treated iTregs maintained significantly higher expression of Foxp3gfp, CD25, CD44, CD62L, CD73, CCR6, and CCR7 levels in the NRG mice. **(Fig. 6J)**. Further, NRG mice that received the TACR1-antagonist-

treated iTreg had increased infiltration of Foxp3rfp^{+} cells in the skin compared to only naïve CD4 T cells or Tregs **(Fig. 6K)**. Together, these results suggest that iTregs differentiated in the presence of TACR1-antagonist are more stable, potent suppressive phenotype and protect from the inflammatory response induced by effector CD4 T cells in the skin and gut.

Discussion

The role of tachykinins in CD4 T cell development is not well understood. Here, we showed TACRs expression in the naïve CD4 T cells, Treg, Th17, and memory CD4 T cells. Among different subsets, Th2 cells showed the highest mRNA expression of TACRs, followed by Th17 and Tregs, whereas Th17 and Th1 showed the highest expression of TACR1, indicating the involvement of tachykinin receptors in CD4 T cell functions. It has been demonstrated that TACR1$^{-/-}$ mice have reduced T cell proliferation (10). In Schistosoma infection, the presence of TACR1 is critical for IFN-γ production from T cells (32). It has been reported that IL-12 increases TACR1 and SP expression in T cells, whereas IL-10 decreases SP production and TACR1 expression in murine T cells (32–34). Allergic-sensitized children show higher SP levels with reduced GATA3 and SOCS3 expression and high production of IFN-γ concentration (35), suggesting its role in Th1/Th2 balance. SP/TACR1 regulates T cell migration by upregulating MIP-1β and α-chemokine expression. The TACR1 mediates migration, which is inhibited by the TACR1 antagonist, CP96345 (36). Our data suggest that gut inflammation induced the SP and TACR1 expression in the GALTs and colon and various subsets of CD4 T cells. In the IL-10$^{-/-}$ mice, TACR1 expression in the lamina propria T cells mediates intestinal inflammation, and blocking of TACR1 can reverse intestinal inflammation, highlighting the importance of TACR1 and SP in mucosal inflammation (37). We showed that TACR1-antagonism alters the Foxp3^{+} Tregs and Th17 cells and works in an intrinsic T cell manner. TGF-β inhibits TACR1 internalization, resulting in increased SP-mediated production of pro-inflammatory cytokines like IFN-γ and IL-17 by intestinal T cells (38). However, this needs to be further examined using CD4-specific TACR1 knockout mice.

TACRs have different cognate ligands; SP shows the highest affinity toward TACR1 (39). SP synthesis can be regulated by various enzymes, including PPTA and PAM. In contrast, degradation can be mediated by various enzymes, including ACE, which cleaves peptide bonds at N- the terminus of the molecule (40). By cleaving SP, these enzymes may regulate their level and activity in CD4 T cells. We showed that Th2, Th17, and Tregs express SP metabolism enzymes and can potentially synthesize or degrade SP levels. SP was also secreted in the culture supernatant during various CD4 T cell subset differentiation, which further substantiates our gene expression data. These results suggested that machinery responsible for the synthesis and degradation of SP exists in CD4 T, and SP can work through TACR1 signaling in an autocrine manner. However, this must be further validated using a CD4 T cell-specific knockout system.

We show increased TACR1 and SP in the spleen, mLN, and colon during DSS-induced colitis, suggesting its involvement in DSS-induced pathology. As TACR1 expression was evident in inflammatory conditions, some studies indicate that environmental inflammatory conditions such as cytokine milieu promote upregulation of TACR1 (6, 41), consistent with our present study. We have observed a significant

upregulation of TACR1 and a reduction in inflammatory cytokines in the presence of TACR1 antagonist. Histopathology suggests that the TACR1 antagonist reduced cellular infiltration in the colon in DSS-treated mice compared to the control group. Similarly, studies have reported that TACR1 expression can be altered in various diseases, including inflammation-related diseases such as rheumatoid arthritis, inflammatory bowel disease, and asthma (1). While TACR1 expression is altered in various conditions, its precise role in disease pathogenesis is still being researched and not fully understood. We showed that IBD and IBS patients' colons have increased TACR1 and TACR2 expression, and human CD4 T cells can be differentiated into the $Foxp3^+$ iTreg in the presence of TACR1 antagonist, suggesting its potential therapeutic application in the clinic. However, further investigation is needed to fully understand the link between TACR1 expression and inflammatory disease conditions.

Tregs mostly impart their suppressive capacity through cell-cell contact, local secretion of inhibitory cytokines, local competition for growth factors, etc. Several studies also suggested an array of receptors responsible for the suppressive function of Treg, such as LAG3, CD73, Helios, PDL-1, and CD62L, etc. (42–46). We found that CP96345 treatment augments the expression of LAP-1, PDL-1, CD62L, Helios, and CD73 on Treg cells, which may impact its suppressive function. Further, we also show that CP96345-treated nTregs maintain better Foxp3 expression when cultured with IL-2 but without TGF-β. Interestingly, we have also noted that CP-treated nTreg promotes naïve CD4 T cell differentiation into the Treg population. One possible explanation for this phenomenon is that CP treatment enhances the expression of LAP-1 in iTreg, potentially contributing to Treg differentiation. However, further experiment is needed to validate this hypothesis. Further, adoptively transferred TACR1 antagonist-treated Treg ameliorates skin and gut inflammation in the immunocompromised mice model. These adoptively transferred Tregs are also persistent. Thus, our findings indicate that antagonizing the TACR1 signaling controls gut inflammation by promoting the differentiation of regulatory $Foxp3^+$ Treg subsets and suggest that TACR1 forms an important therapeutic target to prevent gut inflammation and autoimmunity.

Our result agrees with the previous studies that suggest that the TACR1 antagonist ameliorates gut inflammation. Additionally, we have delineated the modulation of CD4 T cells in the presence of TACR1 antagonists in gut inflammation. Our findings indicate that TACR1 signaling is necessary to respond to inflammatory immune cells such as Th1 and Th17, the effector phenotype ($CD4^+CD44^+ROR\gamma t^+$). Studies have shown that $CCR7^+ROR\gamma t^+$ CD4 T cells play a role in initiating and maintaining gut inflammation by producing pro-inflammatory cytokines, such as IL-17, TNF-α, and IL-22. These cytokines are involved in the recruitment and activation of immune cells in response to gut inflammation and play a role in the pathogenesis of various gut inflammatory disorders, including inflammatory bowel disease (IBD) and celiac disease (47, 48). Similarly, we have also shown a significant increase of $CCR7^+ROR\gamma t^+$ CD4 T cells in Peyer’s patches during inflammation, which might be responsible for migrating inflammatory cells in lymph nodes that contribute to the active disease condition, and antagonizing TACR1 significantly reduced these cells. Antagonizing TACR1 significantly decreases effector cells and increases $Foxp3^+$ regulatory T cell infiltration in Peyer's patches. This regulatory phenotype is more potent and suppressive as they showed enhanced expression of receptors such as CD73, CD62L, LAP-1, GITR, and CTLA4.

Subsequently, TACR1 antagonist treatment reduced proinflammatory cytokines such as IL-17A and IL-17A^{+}IFN-γ^{+} in lamina propria of DSS-treated mice. These findings suggest that TACR1 receptors may play a role in regulating CD4 T cell proliferation towards a more inflammatory phenotype and that blocking these receptors with CP96345 could have therapeutic potential in certain conditions.

Recently, it has been given the importance that the enteric nervous system relays psychological stress to intestinal inflammation and exacerbates the IBD and suggested that stress management could serve to control the IBD (49). Many TACR1 antagonists benefit from depression, stress disorders, and anxiety (50–52). Given the role of the tachykinin system in various pathophysiological processes such as immune, nervous, respiratory, gastrointestinal, urogenital, and dermal systems and its contribution to inflammation, nociception, and cell proliferation (53–56), it has been proposed to have antagonism of TACRs gives clinical benefits in the acute diseases such as COVID19 or chronic diseases such as IBD and psoriasis, or agonism in boosting the immunity in cancer patients. The importance of stress in the gut-inflammation, as reported (49), and our data on the induction of Treg-mediated tolerogenic/anti-inflammatory function of the TACR1 antagonist provide a new mechanistic dimension to therapeutic benefits in the clinic for inflammatory gut and skin diseases.

Materials and Methods

Mice

Six to eight weeks-old wild-type C57BL/6, FoxP3gfp transgenic, FoxP3rfp transgenic, and NRG (RAG1$^{-/-}$IL-2Rγ$^{-/-}$) mice were procured from the Jackson Laboratory (Maine, USA) and bred at NCCS experimental animal facility. All experimental procedures and protocols used were approved by the NCCS Institutional Animal Ethics Committee (Reference ID: EAF/2016/B-256 and EAF/2019/B-358).

Induction of acute colitis

Acute colitis was induced in wild-type C57BL/6 mice by giving them 2% dextran sodium sulfate (DSS; w/v) in the drinking water. The development and progression of colitis were monitored daily for weight loss, loose stool, and bloody diarrhea(57). Mice were given intraperitoneal injections of [Sar9, Met(O_2)^{11})]-Substance P (SP; 5 nM/mouse daily), a highly selective TACR1 agonist, or intraperitoneal injections of CP-96345 (a selective TACR1 antagonist; 2.5 mg/kg twice a day) (58, 59). The Disease Activity Index (DAI) consisted of three criteria: stool consistency, bloody stools, and body weight loss. Each criterion is assigned a numerical score based on the severity of the symptom, with higher scores indicating more severe symptoms. A score of 0 for stool consistency is given for normal stool, 2 for loose stool, and 4 for watery diarrhea. For bloody stool, a score of 0 is given for no bleeding, 2 for slight bleeding, and 4 for gross bleeding. For body weight loss, a score of 0 is given for no weight loss, 1 for weight loss of 1%-5%, 2 for weight loss of 5%-10%, 3 for weight loss of 11%-15%, and 4 for weight loss of > 15%. To determine the overall disease severity, the scores for each of the three criteria are added together for each animal, resulting in a DAI score (60).

Mouse $CD4^+$ T cell culture

Purified naïve $CD4^+CD25^-CD44^-$ cells (1 X 10^5 cells/well) were plated in 0.2 ml 96-well flat-bottomed tissue culture plates coated with anti-CD3ε (10 µg/ml). The culture media was supplemented with soluble anti-CD28 (2 µg/ml). The culture was supplemented with cytokines and blocking antibodies to differentiate naïve $CD4^+$ T cells into specific CD4 T cell lineages. For Th0: purified recombinant mouse IL-2 (10 ng/ml); Th1: purified recombinant mouse IL-12 (10 ng/ml), anti-mouse IL-4 (clone 11B11; 10 µg/ml) and purified recombinant mouse IFN-γ (10 ng/ml); Th2: purified recombinant mouse IL-4 (10 ng/ml) and anti-mouse IFN-γ (XMG1.2; 10 µg/ml); pathogenic Th17: purified recombinant mouse IL-1β (10 ng/ml), purified recombinant mouse IL-23 (10 ng/ml), and iTreg: purified recombinant human TGF-β1 (10 ng/ml). The plates were incubated at 37^oC in a 5% CO_2 incubator for five days. The gene expression and cytokine production were analyzed using flow cytometry (FACS CANTO-II, BD Biosciences) or a Spectral flow cytometer (Cytek Aurora, Cytek).

Intracellular cytokine staining

For cytokine analysis, the cells were stimulated with phorbol 12-myristate 13-acetate (PMA; 81 nM), ionomycin (1.34 µM), and brefeldin-A (10.6 µM) in a complete RPMI medium at 37^0C in a humified 5% CO_2 incubator for 6 hours. Cells were surface-stained using specific antibodies at 4^0C for 30 minutes. Cells were fixed and permeabilized for intracellular cytokine and transcription factors staining using a Foxp3 fixation/permeabilization kit (Biolegend) according to the manufacturer's guidelines. Cells were washed and acquired using a flow cytometer (FACS Canto II; BD Biosciences), and data were analyzed using FlowJo software (TreeStar).

Quantitative real-time reverse transcription PCR (qRT-PCR)

Expression of TACRs and genes required for synthesis and degradation of SP were measured by qRT-PCR using specific primers. Briefly, total RNA was isolated from tissues or specific immune cells using the Trizol reagent (Invitrogen). Purified RNA was treated with Dnase-I and reverse transcribed into cDNA using cDNA synthesis kits using oligo $(dT)_{11-14}$ primers (Applied Biosciences). qRT-PCR was performed using SYBR Green PCR Kit (Thermofisher Scientific) in CFX96 thermal cycler (BioRad). PCR consisted of a denaturing step (95^0C for 15 minutes) followed by 35 cycles of 15 seconds at 95^0C, 20 seconds at 60^0C, 20 seconds at 72^0C. Relative mRNA expression of a specific gene was calculated as follows: $2^{(Ct\ of\ CyclophilinA - Ct\ of\ a\ specific\ gene)}$. The primers used for qRT-PCR are listed in **Supplementary Table 1**.

Human $CD4^+$ T cell isolation and culture

All the human subject study was approved by the Institutional Ethics Committee of the National Centre for Cell Science (Protocol ID: NCCS/IEC/13032014) as well as by the Armed Forces Medical College (Protocol ID: AFMC/IEC/28102014). After obtaining written informed consent, blood samples (10–15 ml)

were drawn from individuals. To isolate peripheral blood mononuclear cells (PBMCs), each blood sample was diluted with an equal amount of phosphate-buffered saline and overlaid onto a Ficoll-Paque PLUS separation medium into SepMate tubes (Cell Signaling Technology). The cells at the plasma/Ficoll interface were collected and washed with PBS containing 2% fetal bovine serum (FBS), followed by a wash with RPMI 1640 medium containing 10% FBS. Cells were stained for fluorescence-conjugated CD4, CD25, and CD45RA mAb. Naïve CD4 T cells ($CD4^+CD25^-CD45RA^+$) were isolated using a flow cytometry sorter (BD FACS ARIA sorter). Purified naïve CD4 T cells (1 $X10^5$ cells/well) were cultured in the anti-CD3ε coated (10µg/ml) flat-bottomed 96 well plates and in the presence of soluble anti-CD28 mAb (2 µg/ml), Recombinant human TGF-β1 (10 ng/ml) with or without SP or CP. Cells were cultured for four days. After four days, cells were stained for CD4, CD25, and Foxp3 using a Permeabilization/Fixation kit (Biolegend) per manufacturer's guidelines and analyzed using flow cytometry.

Flow cytometry analysis.

Flow cytometry data were analyzed using FlowJo software (TreeStar) or OMIQ software (https://www.omiq.ai/). UMAP data analysis was performed using OMIQ software.

High dimensional data analysis

The analysis of high-dimensional data involved several steps using OMIQ software. Initially, gating was performed, followed by subsampling of replicates within each group. Subsequently, Uniform Manifold Approximation and Projection (UMAP) was conducted using an equal number of samples from each group. In UMAP, the parameters included 15 neighbors, a minimum distance of 0.7, 2 components, an Euclidean distance metric, a random seed of 2150, and spectral embedding initialization. Each UMAP visualization represents the concatenated data from all replicates within each group. Further meta-clustering was performed by using FlowSOM. A metacluster represents the expression of specific markers within a particular cell population. A volcano plot visualizes the relationship between p-values derived from a statistical test by comparing different meta-clusters between groups. This specific volcano plot was created using the edgeR platform based on 'R'. The heatmap was used to represent the expression of particular markers on the cell population.

ELISA

IFN-γ, IL-10 and IL-17 ELISA from culture supernatants were performed using a mouse ELISA Max Deluxe kit from Biolegend (San Diego, CA) per the manufacturer's guidelines. SP was measured in the culture supernatant using an ELISA kit (Cayman Chemical Company).

Immunohistochemistry

Spleen, LNs, and colons were harvested and snap-frozen in an OCT medium (Optimal cutting temperature, Sakura Finetek Inc, Torrance, CA). Seven-micrometer-thick sections were cut using cryo-microtome (Thermo Shandon, Thermo Fisher Scientific, Massachusetts, US), fixed with pre-chilled acetone for 10 minutes, washed with cold PBS, and then blocked with 10% horse serum (Himedia) or 10%

goat serum (Thermofisher Scientific) at room temperature for 60 minutes. Sections were washed with PBS and incubated with 1:200 diluted primary antibodies followed by 1:800 diluted secondary antibodies at room temperature in a humidified chamber for 60 minutes. Sections were washed with PBS and mounted with or without a DAPI-containing mounting medium (ElectroMicroscopypy Sciences, Hatfield, and PA). Sections were visualized under a fluorescent microscope (DMI6000B, Leica Microsystems, Germany).

For hematoxylin and eosin staining, paraffin-embedded skin or colon tissues were cut into seven-micrometer-thick sections. These sections were used for Harris hematoxylin (Himedia Laboratories, India) and eosin (Himedia Laboratories) staining as per the manufacturer's guidelines.

Suppression Assay

Splenic naive $CD4^+CD25^+CD44^-Foxp3gfp^-$ T cells were sorted using flow cytometry. Purified $CD4^+$ T cells (1 X 10^5 cells/well) were cultured with anti-CD3ε mAb (10µg/ml) coated flat-bottomed 96 well plates in the presence of soluble anti-CD28 (2 µg/ml) at 37^0C for four days. Cells were differentiated into Tregs in the presence of TGF-β1 (10 ng/ml) and SP or CP96345 (8 µm). After four days of culture, $CD25^+Foxp3gfp^+$ Tregs were isolated and used for suppression assay. *In vitro* suppression assays were performed as described (61). In brief, Naïve effector CD4 T cells were stained with CellTrace Violet (CTV, ThermoFisher Scientific). CD4-iTreg and CD4-nTreg cells were cocultured with CTV-tagged naïve CD4 T cells in the presence of α-CD3e and α-CD28 antibodies-coated dynabeads (0.43 ul/ well; 1:3 bead-to-cell ratio) in 1:1 (50K:50K), 1:2 (25K:50K) and 1:4 (12.5K:50K) Treg to CD4 T cell ratio in U-bottomed 96 well plates for 72 hours. An aliquot of the CTV-tagged CD4 T cells was immediately fixed with 1% paraformaldehyde and used to set the baseline of the undivided cells in the suppression assay. After 72 hours, cells were harvested and stained with α-CD4 mAb and acquired using flow cytometry (BD Biosciences). Data were analyzed using FlowJo software. Suppression was assessed by calculating the percentage of undivided cells.

Isolation of colonic lamina propria cells

Colon was harvested from mice, cleaned by holding with forceps and flushing with a syringe filled with cold PBS, resected residual mesenteric fat tissue, cut into small pieces, and washed in ice-cold 1 PBS. Colon pieces were incubated in 5 ml of pre-digestion solution (1 HBSS containing 5 mM EDTA and 1 mM DTT) at 37 ^{0}C under slow rotation (40 g) in a thermal incubator in a 50 ml tube for 20 minutes. The colon pieces were passed through a 100 µm cell strainer. The remaining colon pieces were cut into 1–4 mm pieces using scissors. Pieces were collected into 50 ml tubes containing 5 ml of digestion solution [Collagenase I (0.1 mg/ml), Collagenase D (0.1 mg/ml), Collagenase IV (0.2 mg/ml), Dispase (0.35 mg/ml), and DNase-I (0.2 mg/ml)]. Tissues were digested by incubating at 37 ^{0}C under slow rotation for 20 minutes. After incubation, a vortex was done intensely for 20 seconds. The digestion media was neutralized by adding RPMI media containing 10% FBS. The colon pieces were passed through a 100 µm cell strainer to separate the cells. Cell suspensions were centrifuged at 400g at 4 ^{0}C for 10 minutes. Cell

pellets were resuspended in RPMI media containing 10% FBS and used for immunophenotyping using spectral flow cytometry (62).

Statistical analysis

Unpaired two-tailed Student's *t*-test was used to compare the two independent groups. One-way ANOVA was used to compare more than two groups. A *p-value* of less than 0.05 was considered statistically significant. The survival curve was formed using the Kaplan-Meier plot, and the p-value was calculated using the log-rank test. All statistical analyses were performed using GraphPad Prism 6 software (GraphPad Software, San Diego, CA).

Limitations of the Study

In this study, we did not use TACR1$^{-/-}$ mice, CD4 or Foxp3-specific conditional deficient mice, or purified cells from these mice to characterize CD4 T cell differentiation with gut inflammation. We used mouse TACR1 shRNA to downregulate the TACR1 in CD4 T cells and *in vitro* differentiation to confirm our findings. A detailed study using TACR1$^{-/-}$ or specific cell- or tissue-specific deficient mice needs to be investigated.

Declarations

Author's contribution: AM and GL conceived and designed the experiments; GL arranged the funding; AM, SK, NH, and MAH performed the experiments and analyzed the data; DK clinically classified and collected the consent and samples; AM and GL wrote the manuscript.

Acknowledgments: GL received a Swarna Jayanti Fellowship (DST/SJF/LSA-01/2017-18) from the Department of Science and Technology, and a research grant from the Science and Engineering Research Board (EMR/2016/007108), Ministry of Science and Technology, Government of India. AM received a Senior Research Fellowship (SRF) from the Department of Biotechnology, SK and NH received an SRF from the Council of Scientific and Industrial Research (CSIR), and MAH received a Junior Research Fellowship from the Indian Council of Medical Research (ICMR), Government of India.

Conflict of interest statement: The authors declare no commercial or financial conflict of interest.

References

1. Mishra A, and Lal G. Neurokinin receptors and their implications in various autoimmune diseases. *Current Research in Immunology.* 2021;2:66-78.
2. Chhatar S, and Lal G. Role of adrenergic receptor signalling in neuroimmune communication. *Current Research in Immunology.* 2021;2:202-17.
3. Halder N, and Lal G. Cholinergic System and Its Therapeutic Importance in Inflammation and Autoimmunity. *Frontiers in immunology.* 2021;12(1236):660342.

4. Dantzer R. Neuroimmune Interactions: From the Brain to the Immune System and Vice Versa. *Physiol Rev.* 2018;98(1):477-504.
5. Huh JR, and Veiga-Fernandes H. Neuroimmune circuits in inter-organ communication. *Nat Rev Immunol.* 2020;20(4):217-28.
6. Steinhoff MS, von Mentzer B, Geppetti P, Pothoulakis C, and Bunnett NW. Tachykinins and their receptors: contributions to physiological control and the mechanisms of disease. *Physiological reviews.* 2014;94(1):265-301.
7. Morelli AE, Sumpter TL, Rojas-Canales DM, Bandyopadhyay M, Chen Z, Tkacheva O, et al. Neurokinin-1 Receptor Signaling Is Required for Efficient Ca(2+) Flux in T-Cell-Receptor-Activated T Cells. *Cell reports.* 2020;30(10):3448-65 e8.
8. Eglezos A, Andrews PV, Boyd RL, and Helme RD. Modulation of the immune response by tachykinins. *Immunol Cell Biol.* 1991;69 (Pt 4):285-94.
9. Lai J-P, Douglas SD, and Ho W-Z. Human lymphocytes express substance P and its receptor. *Journal of Neuroimmunology.* 1998;86(1):80-6.
10. Lambrecht BN, Germonpré PR, Everaert EG, Carro-Muino I, De Veerman M, de Felipe C, et al. Endogenously produced substance P contributes to lymphocyte proliferation induced by dendritic cells and direct TCR ligation. *European Journal of Immunology.* 1999;29(12):3815-25.
11. Pincelli C, Fantini F, Magnoni C, and Giannetti A. Psoriasis and the nervous system. *Acta Derm Venereol Suppl (Stockh).* 1994;186:60-1.
12. Sandoval-Talamantes AK, Gomez-Gonzalez BA, Uriarte-Mayorga DF, Martinez-Guzman MA, Wheber-Hidalgo KA, and Alvarado-Navarro A. Neurotransmitters, neuropeptides and their receptors interact with immune response in healthy and psoriatic skin. *Neuropeptides.* 2020;79:102004.
13. Grimsholm O, Rantapaa-Dahlqvist S, and Forsgren S. Levels of gastrin-releasing peptide and substance P in synovial fluid and serum correlate with levels of cytokines in rheumatoid arthritis. *Arthritis research & therapy.* 2005;7(3):R416-26.
14. Barbosa-Cobos RE, Lugo-Zamudio G, Flores-Estrada J, Becerril-Mendoza LT, Rodriguez-Henriquez P, Torres-Gonzalez R, et al. Serum substance P: an indicator of disease activity and subclinical inflammation in rheumatoid arthritis. *Clin Rheumatol.* 2018;37(4):901-8.
15. Norton CE, Grunz-Borgmann EA, Hart ML, Jones BW, Franklin CL, and Boerman EM. Role of perivascular nerve and sensory neurotransmitter dysfunction in inflammatory bowel disease. *American journal of physiology.* 2021;320(5):H1887-H902.
16. Blum AM, Metwali A, Elliott DE, and Weinstock JV. T cell substance P receptor governs antigen-elicited IFN-gamma production. *American journal of physiology.* 2003;284(2):G197-204.
17. Goode T, O'Connell J, Anton P, Wong H, Reeve J, O'Sullivan GC, et al. Neurokinin-1 receptor expression in inflammatory bowel disease: molecular quantitation and localisation. *Gut.* 2000;47(3):387-96.
18. Patel M, Valaiyaduppu Subas S, Ghani MR, Busa V, Dardeir A, Marudhai S, et al. Role of Substance P in the Pathophysiology of Inflammatory Bowel Disease and Its Correlation With the Degree of Inflammation. *Cureus.* 2020;12(10):e11027.

19. Renzi D, Pellegrini B, Tonelli F, Surrenti C, and Calabro A. Substance P (neurokinin-1) and neurokinin A (neurokinin-2) receptor gene and protein expression in the healthy and inflamed human intestine. *Am J Pathol.* 2000;157(5):1511-22.
20. Morelli AE, Sumpter TL, Rojas-Canales DM, Bandyopadhyay M, Chen Z, Tkacheva O, et al. Neurokinin-1 Receptor Signaling Is Required for Efficient Ca2+ Flux in T-Cell-Receptor-Activated T Cells. *Cell Reports.* 2020;30(10):3448-65.e8.
21. Hargreaves R, Ferreira JC, Hughes D, Brands J, Hale J, Mattson B, et al. Development of aprepitant, the first neurokinin-1 receptor antagonist for the prevention of chemotherapy-induced nausea and vomiting. *Annals of the New York Academy of Sciences.* 2011;1222:40-8.
22. Zakko S, Barton G, Weber E, Dunger-Baldauf C, and Ruhl A. Randomised clinical trial: the clinical effects of a novel neurokinin receptor antagonist, DNK333, in women with diarrhoea-predominant irritable bowel syndrome. *Alimentary pharmacology & therapeutics.* 2011;33(12):1311-21.
23. Kulkarni N, Sonar SA, and Lal G. Plasticity of Th17 and Tregs and its clinical importance as therapeutic target in inflammatory bowel disease. *Indian Journal of Inflammation Research.* 2018;1(1):R2.
24. Kulkarni N, Meitei HT, Sonar SA, Sharma PK, Mujeeb VR, Srivastava S, et al. CCR6 signaling inhibits suppressor function of induced-Treg during gut inflammation. *J Autoimmun.* 2018;88:121-30.
25. Holzer P, and Holzer-Petsche U. Tachykinins in the gut. Part I. Expression, release and motor function. *Pharmacology & Therapeutics.* 1997;73(3):173-217.
26. Shimizu Y, Matsuyama H, Shiina T, Takewaki T, and Furness JB. Tachykinins and their functions in the gastrointestinal tract. *Cellular and Molecular Life Sciences.* 2008;65(2):295-311.
27. Sethi A, Kulkarni N, Sonar S, and Lal G. Role of miRNAs in CD4 T cell plasticity during inflammation and tolerance. *Frontiers in genetics.* 2013;4:8.
28. Stucchi AF, Shofer S, Leeman S, Materne O, Beer E, McClung J, et al. NK-1 antagonist reduces colonic inflammation and oxidative stress in dextran sulfate-induced colitis in rats. *Am J Physiol Gastrointest Liver Physiol.* 2000;279(6).
29. Lal G, Zhang N, van der Touw W, Ding Y, Ju W, Bottinger EP, et al. Epigenetic regulation of Foxp3 expression in regulatory T cells by DNA methylation. *J Immunol.* 2009;182(1):259-73.
30. Shevach EM. Mechanisms of foxp3+ T regulatory cell-mediated suppression. *Immunity.* 2009;30(5):636-45.
31. Clement RL, Daccache J, Mohammed MT, Diallo A, Blazar BR, Kuchroo VK, et al. Follicular regulatory T cells control humoral and allergic immunity by restraining early B cell responses. *Nature Immunology.* 2019;20(10):1360-71.
32. Blum AM, Metwali A, Elliott DE, and Weinstock JV. T cell substance P receptor governs antigen-elicited IFN-γ production. *American Journal of Physiology-Gastrointestinal and Liver Physiology.* 2003;284(2):G197-G204.
33. Calvo CF, Chavanel G, and Senik A. Substance P enhances IL-2 expression in activated human T cells. *The Journal of Immunology.* 1992;148(11):3498-504.

34. Payan DG, Brewster DR, and Goetzl EJ. Specific stimulation of human T lymphocytes by substance P. *J Immunol.* 1983;131(4):1613-5.
35. Herberth G, Daegelmann C, Weber A, Roder S, Giese T, Kramer U, et al. Association of neuropeptides with Th1/Th2 balance and allergic sensitization in children. *Clin Exp Allergy.* 2006;36(11):1408-16.
36. Guo C-J, Lai J-P, Luo H-M, Douglas SD, and Ho W-Z. Substance P up-regulates macrophage inflammatory protein-1β expression in human T lymphocytes. *Journal of Neuroimmunology.* 2002;131(1):160-7.
37. Weinstock JV, Blum A, Metwali A, Elliott D, Bunnett N, and Arsenescu R. Substance P Regulates Th1-Type Colitis in IL-10 Knockout Mice. *The Journal of Immunology.* 2003;171(7):3762-7.
38. Beinborn M, Blum A, Hang L, Setiawan T, Schroeder JC, Stoyanoff K, et al. TGF-β regulates T-cell neurokinin-1 receptor internalization and function. *Proceedings of the National Academy of Sciences.* 2010;107(9):4293-8.
39. Mantyh PW. Neurobiology of substance P and the NK1 receptor. *J Clin Psychiatry.* 2002;11:6-10.
40. Mendlewicz J, Oswald P, Claes S, Massat I, Souery D, Van Broeckhoven C, et al. Patient-control association study of substance P-related genes in unipolar and bipolar affective disorders. *The international journal of neuropsychopharmacology / official scientific journal of the Collegium Internationale Neuropsychopharmacologicum (CINP).* 2006;8:505-13.
41. Williams R, Zou X, and Hoyle GW. Tachykinin-1 receptor stimulates proinflammatory gene expression in lung epithelial cells through activation of NF-kappaB via a G(q)-dependent pathway. *American journal of physiology Lung cellular and molecular physiology.* 2007;292(2):L430-7.
42. Kobie JJ, Shah PR, Yang L, Rebhahn JA, Fowell DJ, and Mosmann TR. T regulatory and primed uncommitted CD4 T cells express CD73, which suppresses effector CD4 T cells by converting 5'-adenosine monophosphate to adenosine. *J Immunol.* 2006;177(10):6780-6.
43. Huang CT, Workman CJ, Flies D, Pan X, Marson AL, Zhou G, et al. Role of LAG-3 in regulatory T cells. *Immunity.* 2004;21(4):503-13.
44. Tan CL, Kuchroo JR, Sage PT, Liang D, Francisco LM, Buck J, et al. PD-1 restraint of regulatory T cell suppressive activity is critical for immune tolerance. *Journal of Experimental Medicine.* 2020;218(1).
45. Thornton AM, Lu J, Korty PE, Kim YC, Martens C, Sun PD, et al. Helios(+) and Helios(-) Treg subpopulations are phenotypically and functionally distinct and express dissimilar TCR repertoires. *Eur J Immunol.* 2019;49(3):398-412.
46. Lange C, Scholl M, Melms A, and Bischof F. CD62L(high) Treg cells with superior immunosuppressive properties accumulate within the CNS during remissions of EAE. *Brain Behav Immun.* 2011;25(1):120-6.
47. McNamee EN, Masterson JC, Veny M, Collins CB, Jedlicka P, Byrne FR, et al. Chemokine receptor CCR7 regulates the intestinal TH1/TH17/Treg balance during Crohn s-like murine ileitis. *Journal of Leukocyte Biology.* 2015;97(6):1011-22.
48. Bishu S, El Zaatari M, Hayashi A, Hou G, Bowers N, Kinnucan J, et al. CD4+ Tissue-resident Memory T Cells Expand and Are a Major Source of Mucosal Tumour Necrosis Factor α in Active Crohn's

Disease. *Journal of Crohn's and Colitis.* 2019;13(7):905-15.

49. Schneider KM, Blank N, Alvarez Y, Thum K, Lundgren P, Litichevskiy L, et al. The enteric nervous system relays psychological stress to intestinal inflammation. *Cell.* 2023.
50. Kramer MS, Cutler N, Feighner J, Shrivastava R, Carman J, Sramek JJ, et al. Distinct mechanism for antidepressant activity by blockade of central substance P receptors. *Science.* 1998;281(5383):1640-5.
51. Ebner K, Sartori SB, and Singewald N. Tachykinin receptors as therapeutic targets in stress-related disorders. *Current pharmaceutical design.* 2009;15(14):1647-74.
52. Mathew SJ, Vythilingam M, Murrough JW, Zarate CA, Jr., Feder A, Luckenbaugh DA, et al. A selective neurokinin-1 receptor antagonist in chronic PTSD: a randomized, double-blind, placebo-controlled, proof-of-concept trial. *European neuropsychopharmacology : the journal of the European College of Neuropsychopharmacology.* 2011;21(3):221-9.
53. Janket SJ, Fraser DD, Baird AE, Tamimi F, Sohaei D, Conte HA, et al. Tachykinins and the potential causal factors for post-COVID-19 condition. *Lancet Microbe.* 2023.
54. Schirinzi T, Lattanzi R, Maftei D, Grillo P, Zenuni H, Boffa L, et al. Substance P and Prokineticin-2 are overexpressed in olfactory neurons and play differential roles in persons with persistent post-COVID-19 olfactory dysfunction. *Brain Behav Immun.* 2023;108:302-8.
55. Bandyopadhyay M, Morelli AE, Balmert SC, Ward NL, Erdos G, Sumpter TL, et al. Skin codelivery of contact sensitizers and neurokinin-1 receptor antagonists integrated in microneedle arrays suppresses allergic contact dermatitis. *The Journal of allergy and clinical immunology.* 2022;150(1):114-30.
56. Restaino AC, Walz A, Vermeer SJ, Barr J, Kovacs A, Fettig RR, et al. Functional neuronal circuits promote disease progression in cancer. *Sci Adv.* 2023;9(19):eade4443.
57. Wang L, Ray A, Jiang X, Wang JY, Basu S, Liu X, et al. T regulatory cells and B cells cooperate to form a regulatory loop that maintains gut homeostasis and suppresses dextran sulfate sodium-induced colitis. *Mucosal Immunol.* 2015;8(6):1297-312.
58. Frederickson RCA, Burgis V, Harrell CE, and Edwards JD. Dual Actions of Substance P on Nociception: Possible Role of Endogenous Opioids. *Science.* 1978;199(4335):1359-62.
59. Bang R, Sass G, Kiemer AK, Vollmar AM, Neuhuber WL, and Tiegs G. Neurokinin-1 receptor antagonists CP-96,345 and L-733,060 protect mice from cytokine-mediated liver injury. *J Pharmacol Exp Ther.* 2003;305(1):31-9.
60. Chen L, Zhou Z, Yang Y, Chen N, and Xiang H. Therapeutic effect of imiquimod on dextran sulfate sodium-induced ulcerative colitis in mice. *PLoS One.* 2017;12(10).
61. Collison LW, and Vignali DA. In vitro Treg suppression assays. *Methods Mol Biol.* 2011;707:21-37.
62. Weigmann B, Tubbe I, Seidel D, Nicolaev A, Becker C, and Neurath MF. Isolation and subsequent analysis of murine lamina propria mononuclear cells from colonic tissue. *Nature Protocols.* 2007;2(10):2307-11.

Figures

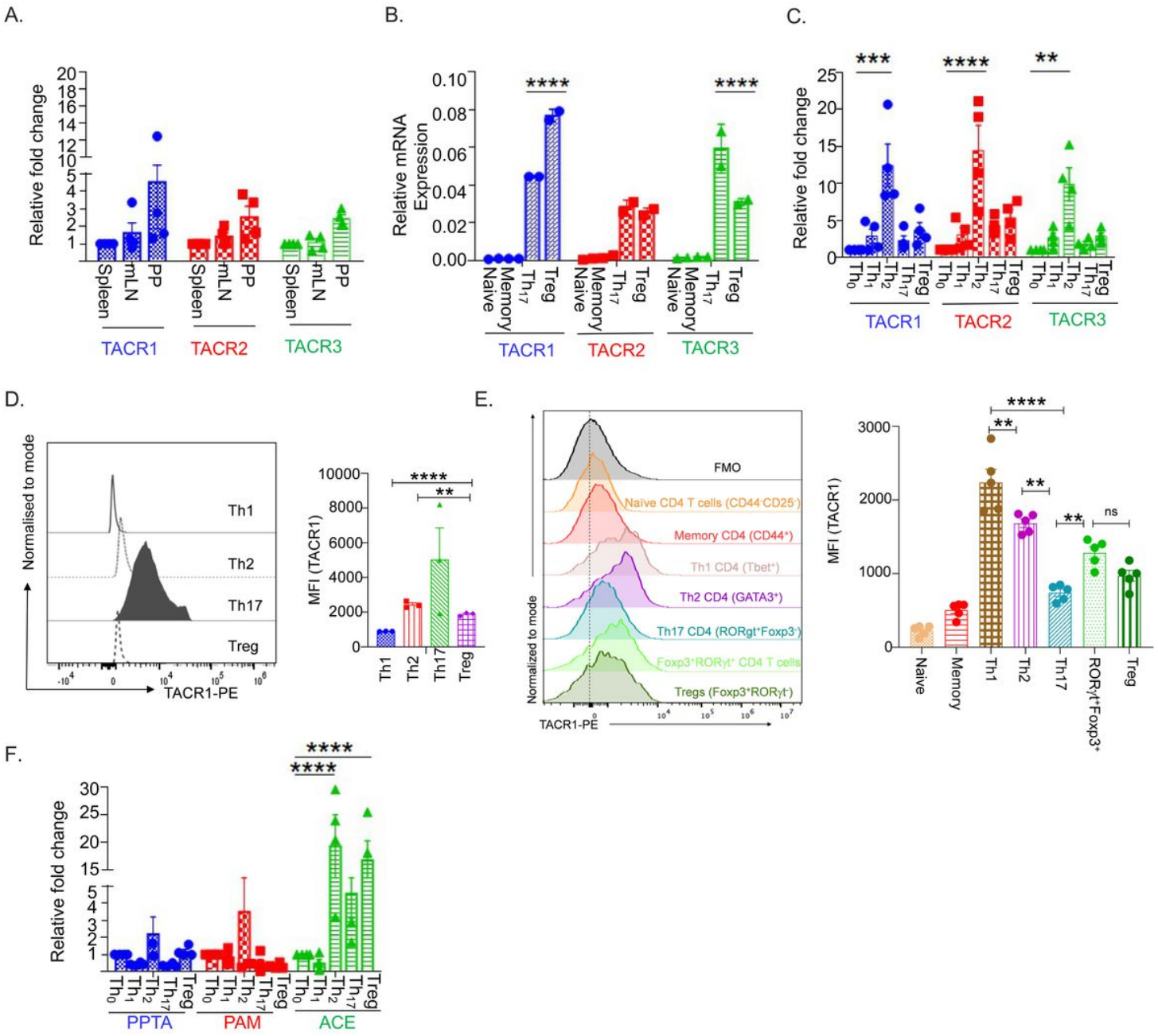

Figure 1

Figure 1

CD4 T cells express TACRs and enzymes required for SP metabolism. (A) qRT-PCR analysis of TACRs mRNA expression in naïve C57BL/6 mice spleen, mesenteric lymph nodes (mLN), and Peyer's patch (PP). **(B)** Naïve CD4 T cells ($CD4^+CD25^-CD44^-$), memory CD4 T cells ($CD4^+CD25^-Foxp3rfp^-CD44^+$), Th17 cells ($CD4^+Foxp3rfp^-RORgtgfp^+$), and natural Treg cells ($CD4^+Foxp3rfp^+RORgtgfp^-$) were isolated from naïve $FoxP3^{rfp/rfp}$::$RORC^{gfp/-}$ mice splenocytes. TACR mRNA expression was analyzed qRT-PCR. **(C)** Naïve CD4 T ($CD4^+CD25^-CD44^-$) cells from naïve C57BL/6 were *in vitro* differentiated into Th1, Th2, Th17 and Treg

lineages. The expression of TACR mRNA was monitored. **(D)** Flow cytometry analysis of TACR1 expression on cultured CD4 T cell subsets. Histogram overlay of TACR1 expression (left) and Mean fluorescence intensity (MFI, right). **(E)** Naïve C57BL/6 mice Peyer's patch CD4 T cells were analyzed using flow cytometry for TACR1 expression after gating on specific markers (left) and MFI (right). **(F)** PAM, PPTA, and ACE mRNA expression were monitored in various CD4 T cell lineages using qRT-PCR. All the data were normalized to GAPDH mRNA. Each symbol represents data from individual experiments (A-D, F; n = 4 experiments). Each symbol represents data from an individual mouse (E; n = 5 mice). Results were analyzed by one-way ANOVA, and the error bar represents the standard error mean. *p < 0.05; **p < 0.01; ***p < 0.001; ****p < 0.0001; ns, not significant.

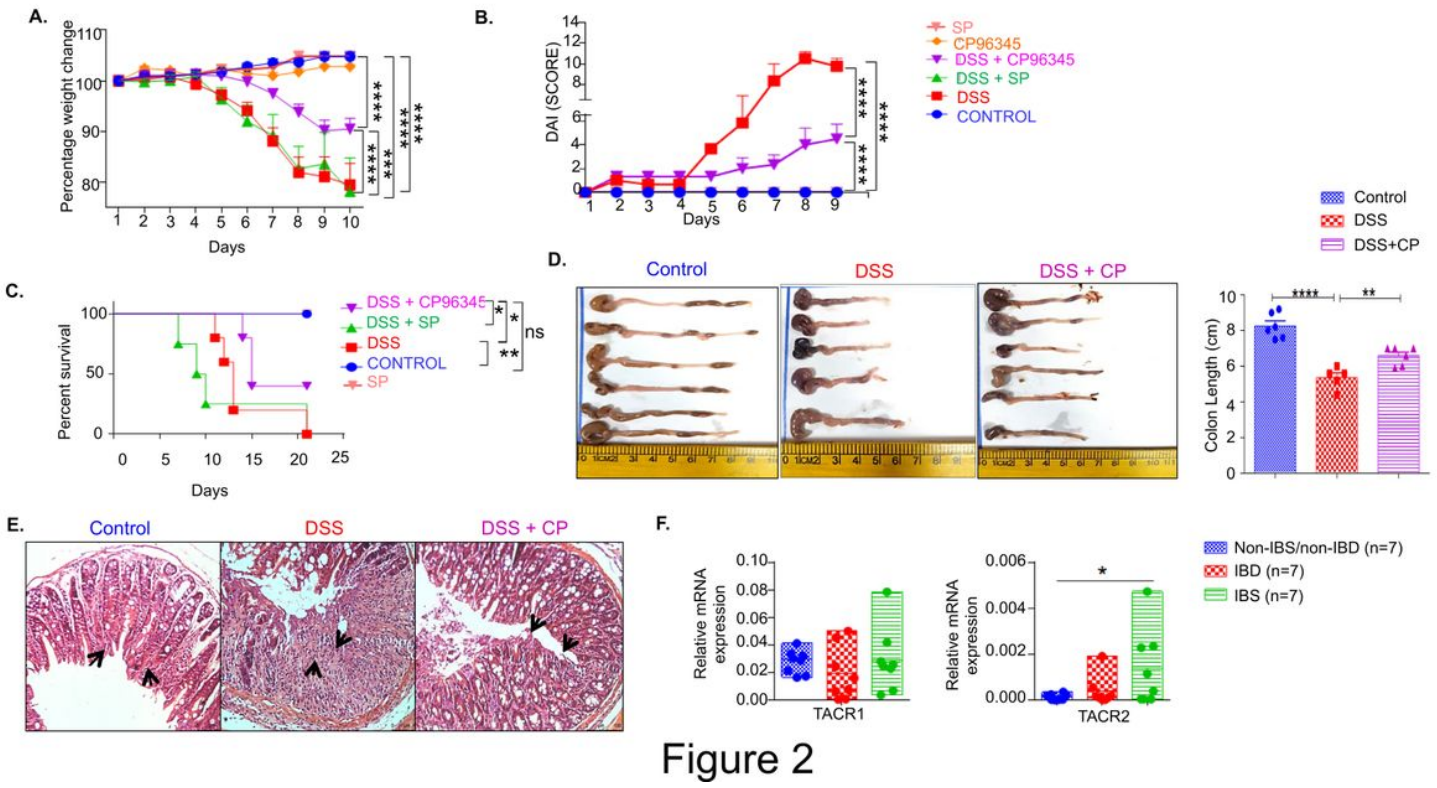

Figure 2

Figure 2

Antagonizing TACR1 ameliorates gut inflammation. Naïve C57BL/6 mice were given 2% DSS in drinking water or DSS and i.p. injection of TACR1 antagonist (CP96345), or TACR1-specific agonist SP [(Sar9, Met(O2)11)-Substance P (trifluoroacetate salt)]. **(A)** The percent weight loss from the original weight is shown. **(B)** The disease activity Index was calculated and shown. **(C)** Mice survival was monitored and presented as a Kaplan-Meier plot, and statistics were calculated using the log-rank (Mantel-Cox) test. **(D)** The colon lengths of different groups on day ten are shown. **(E)**H&E of the colon (200x magnification). **(F)** Colon biopsies were from inflammatory bowel disease (IBD), irritable bowel syndrome (IBS), and non-IBD/non-IBS patients' samples were analyzed for TACR1, TACR2, and TACR3 mRNA expression using qRT-PCR. None of the colonic biopsies showed TACR3 expression (data not shown). Each symbol represents a sample from individual patients (F). Results were analyzed by one-way ANOVA, and the error bar represents the standard error mean.*p < 0.05; **p < 0.01; ***p < 0.001; ****p < 0.0001; ns, not

significant. The result represents one of the three independent experiments (A-E). n = 5-6 mice/group (A-C). n = 7 patients in each group (F).

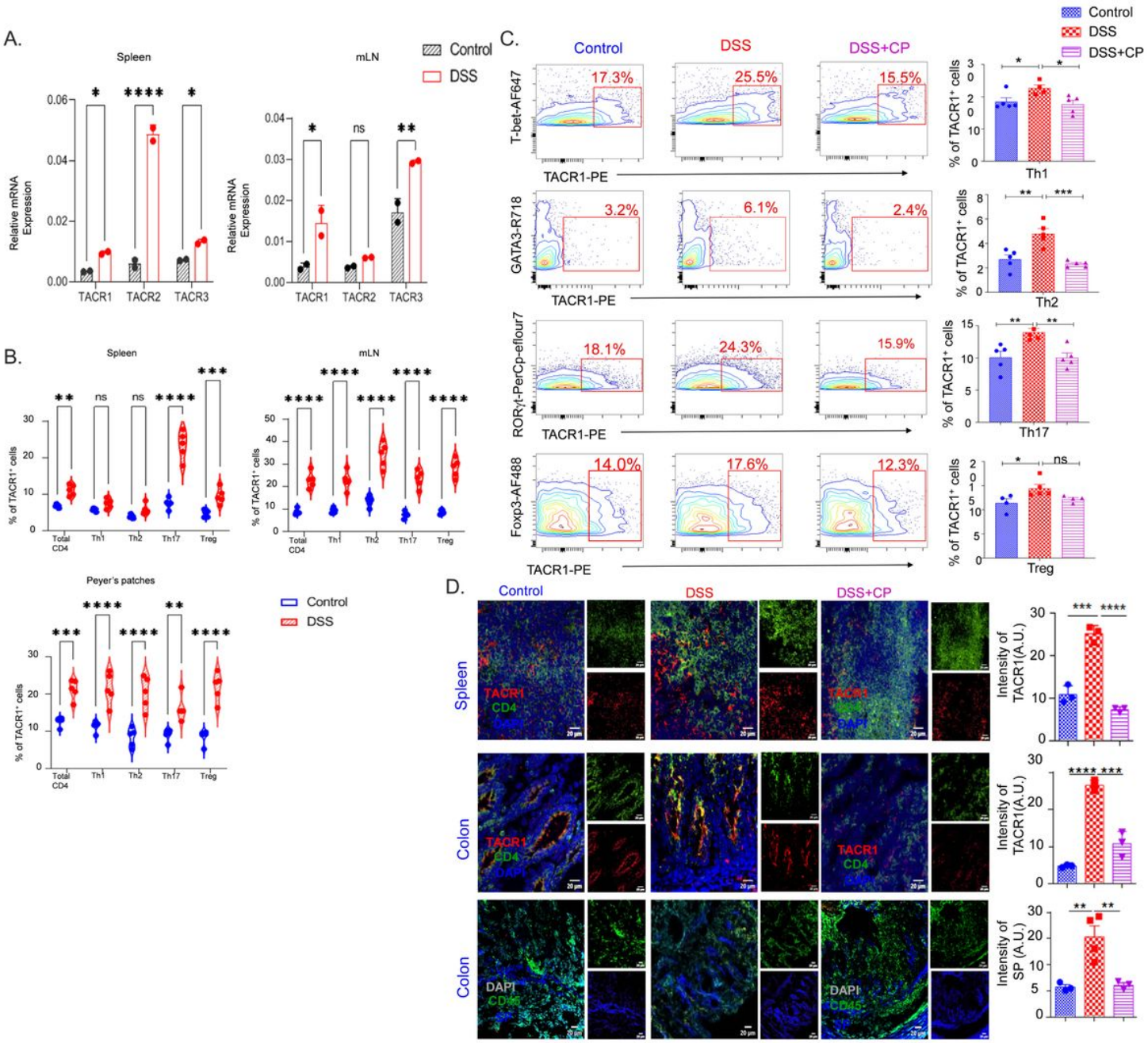

Figure 3.

Figure 3

Gut inflammation increases the TACR1 expression on various subsets of CD4 T cells. C57BL/6 mice were given either 2% DSS in drinking water or plain water as a control. On day 10, mice were sacrificed, and tissues (spleen, mLN, and Peyer's patches) were harvested. **(A)** qRT-PCR analysis of TACRs in the spleen (left) and mLN (right) in mice treated with DSS or control groups. Data were normalized to GAPDH mRNA. **(B)** Cells from the spleen, mLN, and Peyer's patches were stained with CD4 and lineage-specific

transcription factors T-bet, GATA3, RORgt, and FoxP3). TACR1-expressing CD4 T cells of various lineages [Th1 (T-bet$^+$), Th2 (GATA3$^+$), Th17 (RORgt$^+$), and Tregs (Foxp3$^+$)] were analyzed using flow cytometry. The data shows cells gated on CD4$^+$ cells. **(C)** TACR1 expression on various CD4 T cell subsets in the Peyer's patch was analyzed using flow cytometry. The data shows cells gated on CD4$^+$ cells. **(D)** Immunofluorescence staining of spleen and colon tissues shows the expression of TACR1 (red), CD4 (green), and nuclear stain DAPI (blue) (upper and middle panel). Colon tissue sections were stained for SP (blue), DAPI (grey), and CD45 (green) (bottom panel). Small boxes of individual stains are shown at the right of each overlay of the stained section. Original magnification 400X. Signal intensity was calculated and plotted as a bar graph. n = 5-6 mice/group. Results were analyzed using one-way ANOVA; the error bar represents the standard error mean. *p < 0.05; **p < 0.01; ***p < 0.001; ****p < 0.0001; ns, not significant. Each symbol represents data from an individual mouse (A, B, C).

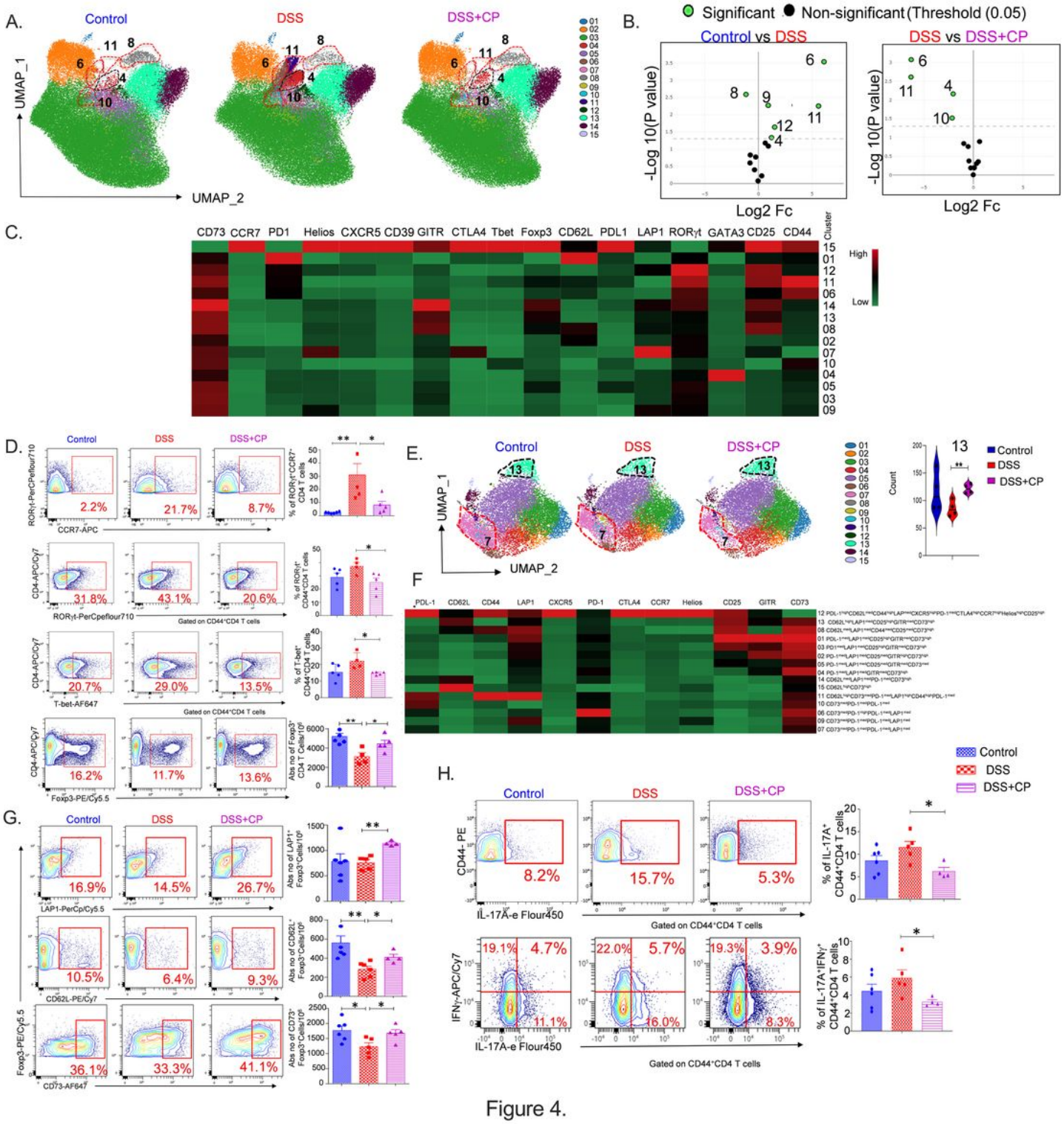

Figure 4.

Figure 4

Antagonizing TACR1 in DSS-induced colitis promotes regulatory CD4 T cells and anti-inflammatory response. C57BL/6 mice were given 2% DSS, DSS plus CP-96345, or DSS plus SP. Mice were sacrificed on day ten, and cells were analyzed for indicated molecules using multi-color spectral flow cytometry. High-dimensional data analysis was performed using OMIQ software. **(A)** UMAP represents different clusters with the unique expression of markers on $CD4^+$ T cells in Peyer's patches. Each meta-cluster represents

the subset of the cell population with a unique pattern of expression of various markers. **(B)** Using edgeR software, a volcano plot was generated to identify differentially regulated immune infiltrate meta clusters among different groups in the Peyer's patches. **(C)** The clustered heatmap was generated to identify the expression of markers in each meta cluster in Peyer's patches. **(D)** A representative contour plot showing RORgt^{+} and CCR7^{+} expression after gating on CD4 T cells in the Peyer's patches. A representative contour plot of CD44^{+} CD4^{+}RORgt^{+}, CD4^{+}CD44^{+}T-bet$^{+,}$ or CD4^{+}Foxp3^{+} cells is shown. The mean percentage of cells was calculated and plotted as a bar graph. **(E)** UMAP represents different clusters with the unique expression of different markers on Foxp3^{+}CD4^{+} T cells (left). Differentially regulated meta-cluster 13 were statistically analyzed using edgeR software and shown as violin plots (right). **(F)** The clustered heatmap was generated to identify the expression of markers in each meta cluster. **(G)** LAP1, CD62L, and CD73 expression on Foxp3^{+}CD4^{+} T cells were analyzed and shown as contour plots (left) and data from individual mice as bar graphs (right). **(H)** CD4^{+}CD44^{+}IL-17A^{+} and IL-17A^{+}IFN-g^{+} CD4^{+}T cells were analyzed and shown as contour plots (left) and data from individual mice as bar graphs (right). Results were analyzed by one-way ANOVA, and the error bar represents the standard error mean (D, E, G, H). Each symbol represents data from individual mice (D, E, G, H). *p < 0.05; **p < 0.01; ***p < 0.001; ns, not significant. n = 5-6 mouse/group. The results shown are representative of one of the two independent experiments.

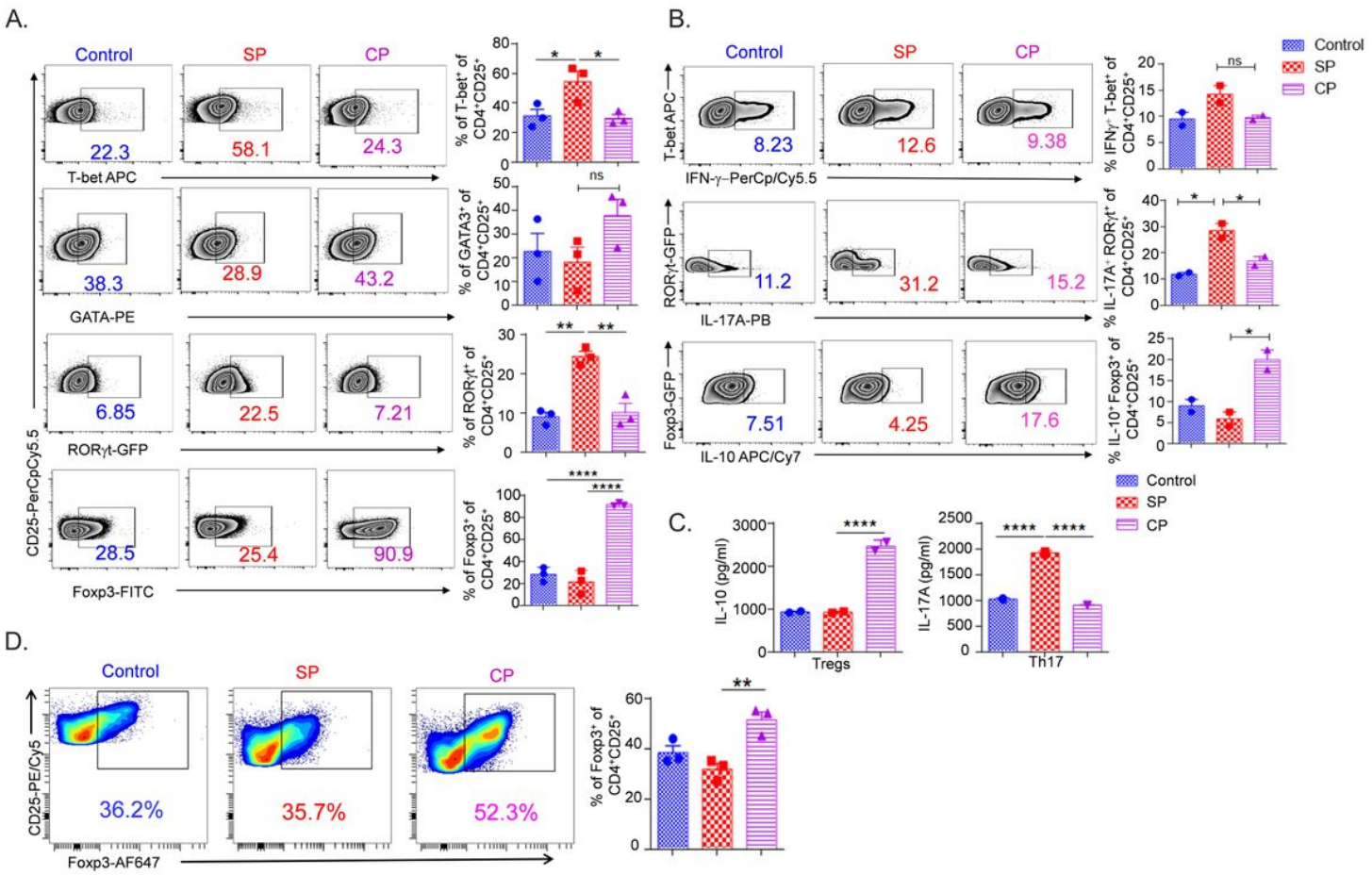

Figure 5.

Figure 5

TACR1 signaling promotes inflammatory Th1 cells, and antagonizing TACR1 drives the differentiation of Th2 and Foxp3$^+$ iTreg cells. Naïve CD4 T ($CD4^+CD25^+CD44^-$) cells were *in vitro* differentiated into Th1, Th2, Th17, and Treg in the presence of SP (10 µm) or CP (8 µm) for four days. **(A)** A representative contour plots of T-bet$^+$ (Th1), GATA3$^+$ (Th2), RORgt$^+$ (Th17), and Foxp3$^+$ (Treg) are shown after gating on $CD4^+CD25^+$ T cells (right). Statistical details are shown as a bar graph (left). **(B)** A representative contour plot of intracellular cytokine secretion of IFN-g, IL-17, and IL-10 is shown after gating on a Th1, Th17, and Treg lineage-specific transcription factor (right). Statistical details are shown as a bar graph (left). Each symbol in the bar graph indicates the mean percentage of cells from one of the experiments. Error bar represents ± SEM, n = 2-3 independent experiments. **(C)** Concentrations of IL-17A and IL-10 in the culture supernatant were measured by ELISA. Data from two experiments in duplicates are shown. **(D)** Naïve human CD4 T cells ($CD4^+CD25^-CD44^-CD45RA^{hi}$ cells) were isolated from PBMC using a flow cytometry sorter and *in vitro* differentiated into Treg lineage in the presence of anti-CD3e, anti-CD28, and TGF-b, and with or without SP or CP. Expression of Foxp3$^+$ was analyzed on $CD4^+CD25^+$ T cells (left). The data shown are from 3 independent cultures and are plotted as a bar graph (right). Each symbol represents data from an individual experiment. One-way ANOVA and the error bar represent the standard error mean.*p < 0.05; **p < 0.01; ***p < 0.001; ****p < 0.0001; ns, not significant.

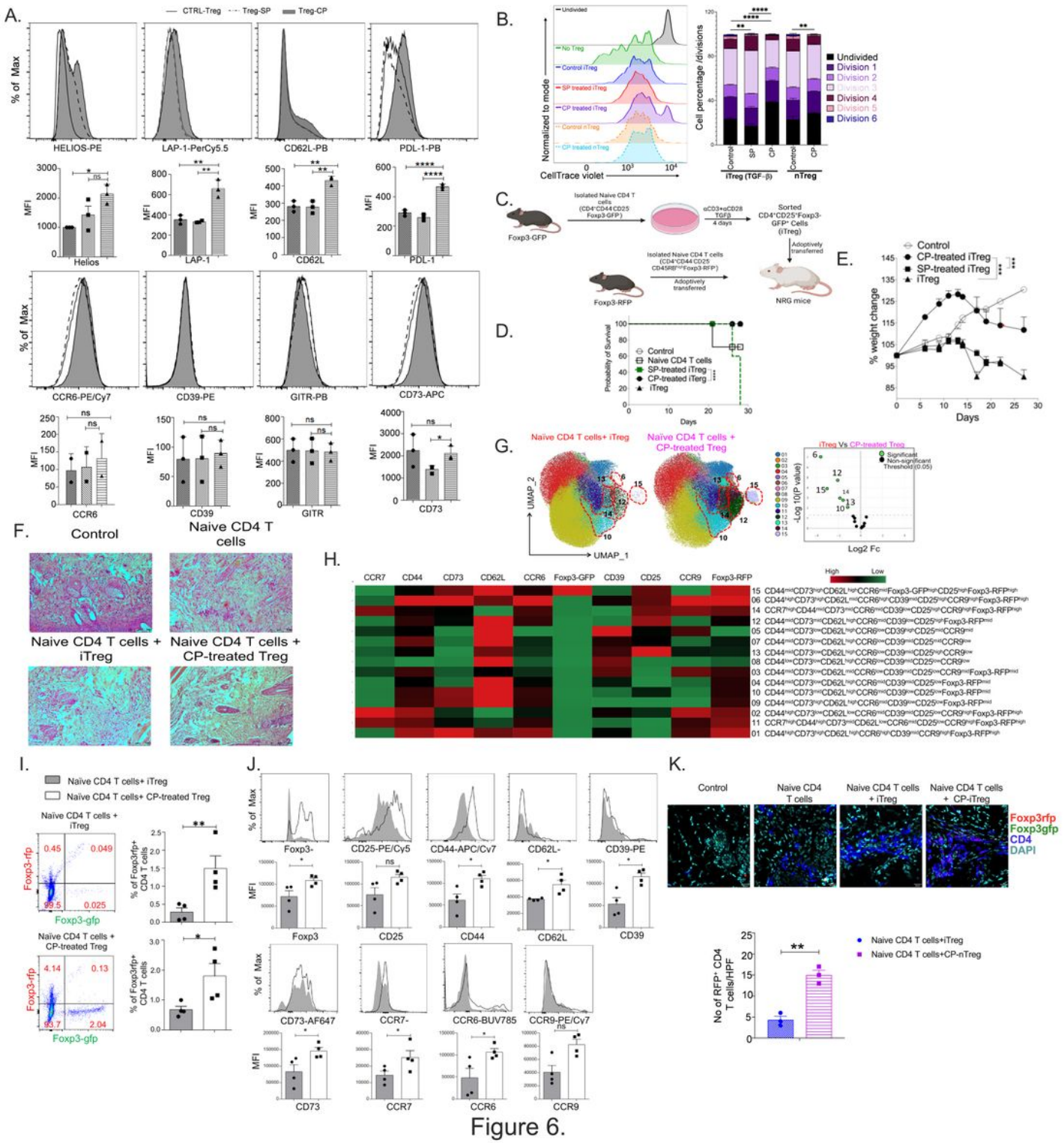

Figure 6.

Figure 6

TACR1 antagonism-treated Foxp3$^+$iTregs suppress the inflammatory skin and gut immune response. Naive CD4$^+$CD25$^+$CD44$^-$ Foxp3gfp$^-$ cells (1 X 10^5 cells/well) were isolated and *in vitro* differentiated into Foxp3gfp$^+$Tregs and nTreg (CD4$^+$CD25$^+$CD44$^+$ Foxp3gfp$^+$) were cultured in the presence CP for 4 days. These cells were further characterized and used for *in vitro* and *in vivo* suppression assay. **(A)** Expression

of various molecules on *in vitro* differentiated Foxp3gfp$^+$ iTregs and plotted as a histogram overlay. Data shown are gated on Foxp3gfp$^+$ CD4$^+$ T cells. The mean fluorescence intensity (MFI) for each marker was calculated and plotted. Each symbol in the bar graph represents data from individual experiments. **(B)** CellTrace violet (CVT) stained CD4$^+$CD25$^-$CD44$^-$ effector T cells were co-cultured with *in vitro* differentiated various groups of Foxp3gfp$^+$ iTregs and CP conditioned nTreg. After four days, the dilution of CVT stain on effector CD4 T cells was analyzed using flow cytometry and shown as a histogram overlay (1:1 ratio) (left). The figure shows a representative of the cell division analysis performed. Statistical comparison is based on percentages of the undivided cells (right). **(C)** Naïve CD4 T cells (CD4$^+$CD25$^-$CD44$^-$CD45RB^{hi}Foxp3rfp$^-$ cells) were adoptively transferred with or without *in vitro* differentiated iTregs (CD4$^+$CD25$^+$Foxp3gfp$^+$) into NRG mice as given in experimental outline. **(D)** The survival of NRG mice that received various types of iTregs was monitored and presented as a Kaplan-Meier plot, and statistics were calculated using the log-rank (Mantel-Cox) test. **(E)** The percent weight loss from the initial weight of mice was calculated and plotted. One-way ANOVA with Tukey's test. **(F)** H&E staining of the back skin of mice was performed. Representative skin tissue is shown. Original magnification 200 X. **(G)** The NRG mice that survived till day 28 were sacrificed, and splenocytes were stained for different molecules on CD4 T cells and acquired using spectral flow cytometry. UMAP represents different clusters with the unique expression of different markers (CCR7, CD73, CD62L, CCR6, CD39, CD44, CD25, CCR9, Foxp3gfp, and Foxp3rfp) on CD4 T cells (right side). Using EdgeR software, a volcano plot was generated to identify differentially regulated immune infiltrate meta clusters among different groups (left). **(H)** The clustered heatmap was generated to identify the expression of markers in each meta cluster on CD4 T cells. **(I)** The frequency distribution of adoptively transferred CP-treated iTregs (Foxp3gfp$^+$) and iTregs (Foxp3rfp$^+$ cells) differentiated from transferred naïve CD4 T cells in NRG mice spleen were analyzed after gating on CD4$^+$ T cells. **(J)** The expression of various markers of control iTregs and CP-treated iTregs in the NRG mice after 28 days of adoptive transfer were analyzed and shown as an overlay. The filled histogram represents the control iTreg, and the empty histogram represents CP-treated iTregs. MFI of different receptors on control iTregs and PC-treated Tregs were analyzed and plotted as a bar graph. **(K)** The distribution of Foxp3gfp (green), Foxp3rfp (red), CD4 T cells (blue), and nuclear stain DAPI (Cyan) in the back skin tissue sections of NRG mice were analyzed using immunofluorescence staining. Original magnification 600X. Representative microscopy images are shown, with a bar graph representing the number of Foxp3rfp$^+$ CD4 T cells in a high-power field (600X)**.** Each symbol represents data from individual mice, B) from individual mice (I, J). Results were analyzed using the Student t-test (A, E, I, J, K). The error bar represents ± SEM (A, B, E, I, J, K). *p < 0.05; **p < 0.01; ***p < 0.001; ****p < 0.0001; ns, not significant. The result represents one of the two independent experiments (D-K). n=3-5 mice/group (D-K).

Supplementary Files

This is a list of supplementary files associated with this preprint. Click to download.

- GraphicalAbstract.jpg
- SupplementaryTable.pdf
- Supplementarymaterials.pdf